Published in final edited form as:
Biomaterials. 2011 May ; 32(15): . doi:10.1016/j.biomaterials.2011.01.073.

Integrin-assisted drug delivery of nano-scaled polymer therapeutics bearing paclitaxel

Anat Eldar-Boock[1], **Keren Miller**[1], **Joaquin Sanchis**[2], **Ruth Lupu**[3], **María J. Vicent**[2,*], and **Ronit Satchi-Fainaro**[1,*]

[1] Department of Physiology and Pharmacology, Sackler School of Medicine, Tel Aviv University, Tel Aviv 69978, Israel

[2] Centro de Investigación Príncipe Felipe, Medicinal Chemistry Unit, E-46012 Valencia, Spain

[3] Mayo Clinic, Mayo Medical Laboratories, Rochester, MN 55905, USA

Abstract

Angiogenesis plays a prominent role in cancer progression. Anti-angiogenic therapy therefore, either alone or in combination with conventional cytotoxic therapy, offers a promising therapeutic approach. Paclitaxel (PTX) is a widely-used potent cytotoxic drug that also exhibits anti-angiogenic effects at low doses. However, its use, at its full potential, is limited by severe side effects. Here we designed and synthesized a targeted conjugate of PTX, a polymer and an integrin-targeted moiety resulting in a polyglutamic acid (PGA)-PTX-E-[c(RGDfK)$_2$] nano-scaled conjugate. Polymer conjugation converted PTX to a macromolecule, which passively targets the tumor tissue exploiting the enhanced permeability and retention effect, while extravasating via the leaky tumor neovasculature. The cyclic RGD peptidomimetic enhanced the effects previously seen for PGA-PTX alone, utilizing the additional active targeting to the $\alpha_v\beta_3$ integrin overexpressed on tumor endothelial and epithelial cells. This strategy is particularly valuable when tumors are well-vascularized, but they present poor vascular permeability. We show that PGA is enzymatically-degradable leading to PTX release under lysosomal acidic pH. PGA-PTX-E-[c(RGDfK)$_2$] inhibited the growth of proliferating $\alpha_v\beta_3$-expressing endothelial cells and several cancer cells. We also showed that PGA-PTX-E-[c(RGDfK)$_2$] blocked endothelial cells migration towards vascular endothelial growth factor; blocked capillary-like tube formation; and inhibited endothelial cells attachment to fibrinogen. Orthotopic studies in mice demonstrated preferential tumor accumulation of the RGD-bearing conjugate, leading to enhanced antitumor efficacy and a marked decrease in toxicity as compared with free PTX-treated mice.

Keywords

Angiogenesis; polymer therapeutics; Polyglutamic acid; paclitaxel; RGD peptidomimetic; integrin

[*]Corresponding Authors: Ronit Satchi-Fainaro, Ph.D. Tel: +972-3-640 7427, Fax: +972-3-640 9113, ronitsf@post.tau.ac.il. María J. Vicent, Ph.D. Tel: +34-963289680, Fax: +34-963289701. mjvicent@cipf.es.

INTRODUCTION

Pharmacological, molecular and genetic evidence demonstrate that tumor progression is angiogenesis-dependent [1, 2]. Cell adhesion mechanisms facilitating migration and invasion through the extracellular matrix are critical to the growth of new blood vessels [3]. Integrins, a class of receptors involved in cell adhesion, play a key role in cell matrix interactions and thus in angiogenesis. Integrin alterations are responsible for a number of pathological manifestations, such as defective embryogenesis, blood coagulation, osteoporosis, acute renal failure, retinopathy and cancer [4, 5].

$\alpha_v\beta_3$ integrin receptors are involved in angiogenesis and tumor invasiveness, essensial in cell adhesion, motility, growth and differentiation [6]. $\alpha_v\beta_3$ integrin binds the Arg-Gly-Asp (RGD) sequence, which constitutes the recognition domain of adhesion proteins including laminin, fibronectin and vitronectin [7]. RGD peptidomimetics compete with extracellular matrix proteins to bind to integrin receptors [8]. $\alpha_v\beta_3$ receptors are expressed mainly on the luminal surface of the endothelial cell predominantly during angiogenesis, making it a compelling target for agents within the vascular space. In addition, $\alpha_v\beta_3$ integrin is overexpressed on proliferating tumor endothelial cells, as well as on various tumor cells, such as glioblastoma [9]. It is a marker of poor prognosis for some tumor types [10, 11]. The bis-cyclic peptide E-[c(RGDfK)$_2$] is a vascular-targeting ligand used in this study to actively and selectively target the chemotherapeutic drug paclitaxel (PTX) to tumor cells and their surrounding tumor endothelial cells via binding to $\alpha_v\beta_3$ integrin receptor.

The microtubule-interfering agent PTX is a clinically well-established and highly-effective anti-neoplastic drug used for the treatment of many carcinomas including prostate, breast, ovarian, and non-small cell lung cancer. It is also the drug of choice for the treatment of metastatic breast carcinoma. In addition to its anti-neoplastic activity, PTX exhibits anti-angiogenic and pro-apoptotic properties [11]. Due to its hydrophobic nature, PTX is solubilized in CremophorEL or ethanol, when used clinically, causing hypersensitivity reactions in addition to the severe side effects associated with PTX itself (such as neurotoxicity). Moreover, PTX's poor pharmacokinetics (short half-life, low selectivity) leads to the fact that only a small amount of the drug localizes in the tumor. An additional limitation of PTX is that it is a substrate of efflux pumps [12], resulting in multiple drug resistance.

One of the most successful approaches to deliver PTX has been the development of an albumin-based PTX nanoparticle named Abraxane® (ABI-007, Celgene Corporation). It was approved by the FDA in 2004 for the treatment of breast cancer after failure of combination chemotherapy for metastatic disease or relapse within 6 months of adjuvant chemotherapy. PTX is physically entrapped in the Abraxane® nanoparticle, leading to enhanced solubility of PTX and thus avoids harmful solubilizing agent [13].

A chemical conjugation of PTX to a carrier could offer pharmacological advantages. Conjugation of PTX with the non-degradable polymer, *N*-(2-hydroxypropyl) methacrylamide (HPMA) copolymer showed improved pharmacokinetics and promising advantages [14]. The use of this strategy failed clinically due to premature release of PTX in the circulation causing a similar toxicity profile as free PTX. Cell Therapeutics Inc. (Seattle) took a different approach conjugating PTX with the biodegradable polyglutamic acid (PGA), OPAXIO™. It showed clinical benefits, such as safety superiority compared to free PTX, in paclitaxel-based cancer treatment alone or in combination with radiotherapy or other small drugs such as cisplatin [15–17].

PGA is a water-soluble multivalent polymer which allows the conjugation of more than one compound or targeting residue within the polymer backbone. It is non-immunogenic, non-toxic, and biodegradable by cathepsin B [18–20], an enzyme that is highly expressed in most tumor tissues [21–24]. In this manuscript we evaluated the anti-angiogenic effect on top of the known antitumor effect of polymer conjugate of PTX. In addition we improved PGA-PTX conjugate's anti-tumor efficiency and widened its clinical applications. We designed and synthesized a PGA-PTX-E-[c(RGDfK)$_2$] conjugate that targets the tumor both (i) **passively** due to the enhanced permeability and retention (EPR) effect by virtue of its size and structure as PGA-PTX conjugate [25], and (ii) **actively** due to integrin binding.

We have characterized an original and superior targeted therapeutic synthetic nanoconjugate named PGA-PTX-E-[c(RGDfK)$_2$] with the potential to target angiogenesis [26, 27] detected by *in vitro* assays on endothelial cells. In addition, we evaluated its antitumor effect on cancer cell lines both *in vitro* and *in vivo* in tumor-bearing mice.

MATERIALS AND METHODS

Materials

All chemicals and solvents were A.R. grade or purified by standard techniques. Chemical reagents were purchased from Sigma-Aldrich (Madrid, Spain). HPLC grade solvents were from Merck (Barcelona, Spain). PTX was from Petrus Chemicals and Materials Ltd. (Israel) and Shaanxi Sciphar Hi-Tech Industry Co. (Xi'an, China). E-[c(RGDfK)$_2$] and c(RADfK) were from Peptides International (KY, USA). Fluorescence dye Oregon Green cadaverine (OG) was from Invitrogen (Barcelona, Spain). Cy5.5 dye was kindly provided by Prof. D. Shabat (Tel Aviv University, Israel). All tissue culture reagents were purchased from Biological Industries Ltd (Beit Haemek, Israel), unless otherwise indicated.

Chemical data

All reactions requiring anhydrous conditions were performed under an argon or nitrogen atmosphere. Thin layer chromatography (TLC): silica gel plates Merck 60 F254; compounds were visualized by irradiation with UV light and/or by treatment with a solution of phosphomolybdic acid (20 % wt. in ethanol) or with ninhydrine (10 % wt. in ethanol), followed by heating. Size exclusion chromatography (SEC; Shephadex G25 resin, eluent H_2O) analysis was performed using a Viscotek TDA™ Triple detector system, with two TSK-gel columns in series (G3000 PWXL and G2500 PWXL) as well as a guard column (PWXL Guardcol). A flow rate of 0.8 mL/min, and a mobile phase 0.1 M PBS buffer were used. Viscotek Instrument software was employed for data analysis. HPLC was performed using a Merck Hitachi L-2130 HPLC pump and an L-2200 autosampler with a Lichrospher® 100 C18 (150 × 3.9 mm) column. The mobile phase was composed of different acetonitrile gradients in water, containing all of them a final concentration of 0.1 % TFA. The UV spectra were recorded on a Jasco V-530 UV/Vis spectrophotometer. Most of the polymer conjugates were purified by SEC in PD10 pre-packed columns (GE Healthcare, Buckinghamshire, UK) using water as eluent.

Chemical reagents included: N,N-Diisopropylcarbodiimide (DIC), 1-hydroxybenzotriazol (HOBt), di-isopropylethylamine (DIEA), N-hydroxysuccinimide (OHSuc), N,N-dimethylaminopyridine (DMAP) and anhydrous dimethylformamide (DMF).

Ethics Statement

All animal procedures were performed in compliance with Tel Aviv University and Mayo Clinic guidelines, approved by the Institutional Animal Care and Use Committee.

Cell culture

U87-MG human glioblastoma, 4T1 murine breast cancer and human umbilical vein endothelial cells (HUVEC) were obtained from the American Type Culture Collection (ATCC). mCherry-labeled-U87-MG cells were obtained by infection with a pQC-mCherry retroviral vector as previously described [28]. U87-MG cancer cells were grown in Dulbecco's modified Eagle's medium (DMEM) supplemented with 10% fetal bovine serum (FBS), 100 mg/mL Penicillin, 100 U/mL Streptomycin, 12.5 U/mL Nystatin, and 2 mM L-glutamin. 4T1 cells were grown in RPMI-1640 supplemented with 10% FBS, 100 mg/mL Penicillin, 100 U/mL Streptomycin, 12.5 U/mL Nystatin, 2 mM L-glutamin, 1% Hepes 1M, 22.5% Glucose and 1 mM Sodium Pyruvate. HUVEC were cultured in EGM-2 medium (Lonza, Switzerland). All Cells were grown at 37°C; 5% CO_2.

Synthesis of PGA-PTX-E-[c(RGDfK)$_2$] and PGA-E-[c(RDGfK)$_2$] conjugates

PGA was synthesized via N-Carboxyanhydride (NCA) polymerization of glutamic acid as previously described [29].

A. Synthesis of PGA-PTX-peptide conjugates: PGA-PTX-E-[c(RGDfK)$_2$] or PGA-PTX- c(RADfK)—The PGA-PTX-E-[c(RDGfK)$_2$] conjugate was prepared using a two-step synthesis: We initially conjugated PTX with PGA (Mw 17800, Mw/Mn 1.3) by carbodiimide coupling. The reaction was allowed to proceed at room temperature (RT) for 24 h. Thin layer chromatography (TLC, silica) showed complete conversion of the PTX (R_f=0.6) to a polymer conjugate (R_f=0, CH_2Cl_2/MeOH=90:10). Then, without product isolation, OHSuc (30 mol %) was added to the reaction mixture in order to activate the necessary carboxylic groups in the polymer chain for subsequent conjugation of the peptide. The activation of the –COOH groups in the polymer main chain avoids side-reactions (and therefore cross-linking products) with the two –COOH from the aspartic acid peptidic moieties. The reaction was allowed to proceed for 24 h. It was then terminated by pouring the mixture into $CHCl_3$:Acetone. The resulting precipitate was collected and washed again with acetone and MeOH in order to remove the unreacted OHSuc, then collected again and dried in vacuum to yield a white solid powder. The $CHCl_3$:acetone mixture was reserved in order to determine total drug loading (PTX) by HPLC, using indirect measurement. The solid intermediate was dissolved once more in anhydrous DMF and the E-[c(RGDfK)$_2$] or c(RADfK) peptide was conjugated with PGA through a peptidic linker using DMAP as base catalyst and the pH was adjusted to 8 with DIEA. The reaction was allowed to proceed at RT for 48 h. TLC showed complete conversion of E-[c(RGDfK)$_2$] or c(RADfK) (R_f=0.3) to the polymer conjugate (R_f=0, AcOH:MeOH=1:99). To stop the reaction, the mixture was poured into $CHCl_3$:Acetone. The resulting precipitate was collected and dried in vacuum to yield the desired polymer-drug conjugate. The supernatant was kept in order to determine total peptide loading E-[c(RGDfK)$_2$] or c(RADfK) by HPLC, using indirect measurement. The sodium salt of the conjugate was obtained by dissolving the product in 1.0 M $NaHCO_3$. This aqueous solution was purified by SEC (Sephadex G25), removing low molecular weight contaminants and salt excesses. Lyophilization of the fractions yielded the product as a white powder (70–80% yield). PGA was used as multivalent polymeric precursor. In order to keep an appropriate PTX loading, a maximum of 5 mol % E-[c(RGDfK)$_2$] or c(RADfK) loading was considered. The total PTX content in these polymeric conjugates was determined by UV (λ = 227 nm and 230 nm, calibration curve carried out at RT in MeOH) and HPLC (indirect analysis determining PTX content in reaction residues λ = 227 nm, from 35 to 80% of acetonitrile in 25 min, t_R = 10.8 min) and was in the functionalization range of 6.7–8.6 mol%. The total peptide content in these polymeric conjugates as determined by UV (λ = 254 nm and 260 nm, calibration curve carried out at RT in MeOH), HPLC (indirect analysis determining peptide content in reaction residues, flow rate of 1 mL/min using an acetonitrile gradient in aqueous 0.1% TFA from 10 to 90% of acetonitrile in 29 min, λ = 220

nm. The retention time was t_R = 8.0 min for E-[c(RGDfK)$_2$], t_R = 5.3 min for c(RADfK) and t_R = 16.3 min for PTX in these conditions. To determine peptide content by amino acid analysis, 3 mg of each conjugate synthesized were hydrolyzed with 6N HCl at 160°C for 4 h. Samples were then lyophilized and analyzed by LC-MS at Parc Cientific Barcelona Peptide Service (Barcelona, Spain). The amino acid content was found to be in the functionalization range of 4.8–5.6 mol%.

B. Synthesis of PGA-peptide conjugates: PGA-E-[c(RDGfK)$_2$] and PGA-c(RADfK)—PGA was dissolved in anhydrous DMF under nitrogen atmosphere and activated by using OHSuc (24 h reaction). PGA-OSuc was isolated by precipitation in $CHCl_3$ and washed with acetone and methanol. E-[c(RGDfK)$_2$] or c(RADfK) was conjugated through succinimidyl-activated esters to the PGA in DMF. The reaction was allowed to proceed for 48 h at RT. TLC showed complete conversion of E-[c(RGDfK)$_2$] or c(RADfK) (R_f=0.3) to the polymer conjugate (R_f=0, AcOH:MeOH=1:99). To stop the reaction, the mixture was poured into $CHCl_3$:Acetone (4:1). The resulting precipitate was collected and dried in vacuum to yield the desired polymer-peptide conjugate. The supernatant was reserved so as to determine the total peptide mimetic loading by HPLC using indirect measurement. The sodium salt of PGA-E-[c(RGDfK)$_2$] or PGA-c(RADfK) conjugate was obtained by dissolving the product in 1.0 M $NaHCO_3$. This aqueous solution was purified by SEC (Sephadex G25) using water as mobile phase to remove low molecular weight contaminants and salt excesses. Lyophilization of the fractions yielded the product as a white powder (70–80% yield). UV spectroscopy was used to determine the peptide content of the conjugate. In order to characterize the E-[c(RGDfK)$_2$] or c(RADfK) loading on the conjugates a calibration curve was carried out in MeOH at RT, at a maximum absorbance of 260 nm and 254 nm. Also, HPLC (indirect analysis determining peptide content in reaction residues λ = 220 nm, flow rate at 1 mL/min using an acetonitrile gradient in aqueous 0.1 % TFA, a gradient from 10 to 90% of acetonitrile in 29 min was used, t_R = 8.0 min for E-[c(RGDfK)$_2$] and t_R = 5.3 min in the case of c(RADfK)) and amino acid analysis were used to further prove peptide loading (range 4.8–5.6 mol%).

Free drug and peptide content determination by HPLC

Two different extraction procedures were followed in order to determine free drug content in the conjugates synthesized.

a. Aqueous solutions of the conjugates synthesized (1 mg/mL) were prepared, an aliquot (100 μL) was added to a polypropylene tube and made up to 1 mL with water. Then, $CHCl_3$:Acetone (4:1, 5 mL) was added. Samples were then thoroughly extracted by vortexing (3 × 10 sec). The upper aqueous layer was carefully removed and the solvent evaporated. The dry residue was dissolved in HPLC grade methanol (200 μL). In parallel, the same procedure was carried out for the parent compound (PTX or peptides) (using 200 μL of a 1 mg/mL stock solution). The addition of MeOH (1 mL) to re-dissolve the product gave a 200 μg/mL stock from which a range of concentrations was prepared (2 to 100 μg/mL).

b. Aqueous solutions of the conjugates synthesized (1 mg/mL) were prepared and an aliquot (100 μL) was washed by a pre-made RP column with C18 Poros50 resin using MeOH:AcCN mixtures as eluents. The solvent was evaporated and the dry residue was dissolved in HPLC grade methanol (200 μL). The same procedure was carried out for the parent compound (PTX or peptides, using 200 μL of a 1 mg/mL stock solution). The addition of MeOH (1 mL) to re-dissolve the product gave a 200 μg/mL stock from which a range of concentrations was prepared (2 to 100 μg/mL).

The amount of free drug in the conjugates was determined by HPLC using a Lichrospher® C18 (150 × 3.9 mm) column. The flow rate of 1 mL/min was measured using an acetonitrile gradient in aqueous 0.1 % TFA (to simultaneously determine PTX and the peptides, a gradient from 10 to 90% of acetonitrile in 29 min was used). The retention time was t_R = 16.9 min for PTX, t_R = 8.0 min for E-[c(RGDfK)$_2$], t_R = 5.3 min for c(RADfK) (λ = 220 nm).

Synthesis of labeled conjugates (Oregon Green and Cyan conjugation)

A fluorescence probe, Oregon Green-cadaverine (OG) or a NIR-probe, an amino functionalized Cyan 5.5 (Cy5.5), was conjugated to PGA conjugates through free carboxylic groups, in order to study the cellular uptake and trafficking in HUVEC and cancer cells in the case of OG; and for the use of intravital non-invasive imaging for the Cy5.5. The conjugates were dissolved in the minimum amount of anhydrous DMF, then DIC (N,N-diisoproprylcarbodiimmide) and HOBT (1-hydroxybenzotriazole) were added, using DIC/HOBT/COOH groups at molar ratio of 1.5:1.5:1. Subsequently, a DMF solution of the desired probe was added with a Probe/COOH group molar ratio of 1% mol or 2% mol for OG and Cy5.5, respectively. The reactions were monitored by TLC eluted with MeOH. Finally, the DMF was evaporated by vacuum, the residues were re-dissolved with $NaHCO_3$ (1.5:1 molar ratio with COOH groups) and loaded in PD10 column eluted with water, collecting fractions of 1 mL. Each fraction (2 μL) was taken and added to MeOH (498 μL or 998 μL for OG and Cy5.5, respectively), in order to measure the fluorescence and to identify the fractions containing the labeled PGA conjugates and also to quantify the amount of conjugated probe. OG loading ranged from 0.5 to 0.9 mol% and Cy5.5 loading was determined to be quantitative in all cases.

Determination of mean hydrodynamic diameter of the conjugates

DLS measurements were performed at 25°C using a Malvern Zetasizer NanoZS instrument, equipped with a 532 nm laser at a fixed scattering angle of 90°. Polymer conjugate solutions (1 mg/mL) were prepared in PBS pH 7.4. The solutions were sonicated for 10 min and filtered through a 0.22 μm cellulose membrane filter and left 8 h at 4 °C before analysis. Micelle size distribution by volume was measured (diameter, nm) for each conjugate (n≥3).

Drug release profile and polymer degradation kinetics

Mimicking lysosomal conditions: Degradation in the presence of Cathepsin B —Cathepsin B (5 U) was added last to a solution of nanoconjugate, PGA control or free drug (3 mg/mL in a fresh prepared buffer made of 20 mM sodium acetate, 2 mM EDTA and 5 mM DTT, pH 6) and incubated at 37°C. Aliquots (100 μL) were taken at different times up to 72 h, immediately frozen in liquid nitrogen and stored in darkness. The amount of released compound was assayed by HPLC (analysis after extraction procedure by Poros50 resin drug content analysis (λ =227 nm)) and/or by Gel permeation chromatography (GPC, direct analysis) using doxycycline as internal standard. For non-enzymatic hydrolytic cleavage assessment, polymers were incubated in buffer alone in the absence of cathepsin B. Additionally, an LC-MS analysis of the released compounds was carried out to determine the major metabolites released. For the GPC analysis (Viscotek TDA detector), 50 μL aliquots were diluted up to 200 μL with PBS and the % Mw loss with time was determined.

Plasma stability—Conjugates (3 mg/mL) were incubated at 37°C in freshly extracted serum from Wistar rats for up to 24 h. At scheduled times, samples of 100 μL were collected; 15 μL of 0.2 mg/mL solution of doxycycline in MeOH, as internal standard, and 135 μL of MeCN were added to each sample in order to precipitate serum proteins.

Following centrifugation (14000 rpm, 5 min), supernatants were analyzed by HPLC as reported above.

Red blood cells (RBC) lysis assay

2% w/w rat RBC solution was incubated with serial dilutions of PGA-PTX-E-[c(RGDfK$_2$)], PGA-PTX, PGA, and PTX vehicle (Ethanol:CremophorEL:Saline 1:1:8) for 1 hour at 37°C. Negative controls were PBS and Dextran (MW ~70000) while positive controls were 1% w/v solution of Triton X100 (100% lysis) and polyethileneimine (PEI). Following centrifugation, the supernatant was drawn off and its absorbance measured at 550 nm using a microplate reader (Genios, TECAN). The results were expressed as percentage of hemoglobin released relative to the positive control (Triton X100).

$\alpha_v\beta_3$ integrin expression

Cells were harvested with 2.5 mM EDTA, re-suspended in serum-free medium and incubated for 30 min. Cells were then re-suspended in PBS (containing Mg^{2+} and Ca^{2+}) with MAB1976-anti-$\alpha_V\beta_3$ integrin antibody (Chemicon) and incubated for 1 h at RT. Control tubes were antibody-free. Cells were then washed and incubated with FITC-donkey anti-mouse IgG antibody (Jackson) for 30 min at RT, in darkness. Cells (1×10^5) were collected by fluorescence-activated cell sorter (FACS), and analyzed using WinMDI software (6Cytek DxP 6-Color Upgrade, Facscan™).

Semi-quantitative RT-PCR

Total RNA extraction from 4T1 cancer cell lines was performed using the "EZ-RNA" kit according to the manufacturer's instructions (Biological Industries, Beit Haemek Israel). The Reverse Transcriptase reaction was performed with the "EZ-first strand cDNA synthesis kit" using oligo(dT) primers. PCR reactions were carried out using PCR-Ready™ High Specificity (Syntezza) in an ATC 401 thermocycler (Apollo, CLP). To obtain semi-quantitative results, the number of cycles for each reaction was calibrated and kept to a minimum. M109 cDNA was used as a positive control [30]. PCR primers: Mouse β3 Integrin: 5′-AAGCACTGGGTGGTGATTG -3′, 5′-TGAGGTCAAGGTGTGTGA -3′; GAPDH (mouse): 5′-CCATCACCATCTTCCAGGAGC -3′, 5′-GGCATGGACTGTGGTCATGAG -3′. Mouse αv Integrin: 5′-GGACACCGCTCCTCCTGGGT -3′, 5′-CCGGCGGCTGGATGAGCATT -3′.

Intracellular uptake of OG-labeled-PGA conjugates

In vitro: Flow cytometry analysis—HUVEC (5×10^5 cells) were plated and following 24 h were exposed to PGA-OG, PGA-c(RADfK)-OG or PGA-E-[c(RGDfK)$_2$]-OG diluted in EGM-2 medium for 5, 10 or 15 min. Cells were then washed with PBS, harvested with 2.5 mM EDTA, then sorted and analyzed using the ImageStream 100 and the IDEAS software (Amnis Corp., USA).

In vitro: Confocal microscopy—U87-MG cells were seeded on cover glasses for 24 h, then incubated with OG-labeled PGA-E-[c(RGDfK)$_2$] or PGA-c(RADfK) conjugates (50 μM-RGD-equivalent concentration) for 1 h, washed with cold PBS, fixed with 3.5% paraformaldehyde (PFA) for 20 min at RT and washed with PBS again. Cells were then permeabilized with 0.1% Triton-X100 for 5 min, and rinsed with PBS. Actin filaments were labeled with phalloidin-TRITC conjugate (50 mg/mL, 40 min at RT). Cellular uptake of the OG-labeled PGA-E-[c(RGDfK)$_2$] conjugate was monitored utilizing a Zeiss Meta LSM 510 confocal imaging system.

In vivo: Whole mount confocal microscopy—SCID male mice were inoculated s.c. with 2×10^6 mCherry-labeled-U87-MG [28]. Body weight and tumor size were monitored three times a week. Mice bearing tumors at an average volume of 175 mm^3 were injected i.v. with PGA-E-[c(RGDfK)$_2$]-OG or with PGA-E-c(RADfK)-OG (50 μM-RGD-equivalent dose) (n=3 mice/group). One hour following injection, tumors were removed, dissected into thin slices and examined under the Zeiss Meta LSM 510 confocal imaging system.

Endothelial cell adhesion assay

The ability of free and PGA-conjugated E-[c(RGDfK)$_2$] peptides to bind $\alpha_v\beta_3$ expressed on cell surface was evaluated by its capacity to inhibit cell adherence to fibrinogen [31]. HUVEC were harvested with 2.5 mM EDTA and re-suspended in EBM-2, then incubated (30 min, RT) with PTX, PGA, c(RADfK), and E-[c(RGDfK)$_2$], combinations thereof, and with PGA-PTX-c(RADfK) and PGA-PTX-E-[c(RGDfK)$_2$] conjugates. Treated HUVEC (5×10^4 cells/well) were allowed to attach to fibrinogen-coated plates for 1 h at 37 °C. Following incubation, attached cells were fixed with 3.7% formaldehyde, stained with 0.5% crystal violet and imaged using a Nikon TE2000E inverted microscope. The number of attached cells was quantified with NIH ImageJ software. Non-specific binding was determined by adhesion to Bovine Serum Albumin-coated plates.

Cell proliferation assay

HUVEC (1.5×10^4 cells/well) or 4T1 (4×10^3 cells/well) were plated onto 24-well plates, U87-MG cells were plated onto 96 well plates (4×10^3 cells/well). Following 24 h, cells were exposed to PTX, PGA, E-[c(RGDfK)$_2$], c(RADfK), combinations thereof, and with PGA-PTX-E-[c(RGDfK)$_2$] and PGA-PTX-c(RADfK) conjugates (dissolved in the cells' suitable medium, EGM-2 for HUVEC, RPMI or DMEM for cancer cells) at serial concentrations for 72 h treatment. Following incubation, HUVEC and 4T1 cells were counted by Coulter Counter (Beckman Coulter), and U87-MG cells' viability was assessed using XTT reagent.

Migration assay

Cell migration assay was performed as previously described [27]. HUVEC (1.5×10^5) were exposed to PTX, PGA, E-[c(RGDfK)$_2$] and c(RADfK), combinations thereof, and PGA-PTX-E-[c(RGDfK)$_2$] and PGA-PTX-c(RADfK) conjugates, that were added to the upper chamber of transwells for 2 h of incubation prior to migration toward vascular endothelial growth factor (VEGF). Migration was normalized, with 100% representing migration to VEGF alone.

Capillary-like tube formation assay

In vitro capillary-like tube formation of HUVEC was assessed as before [14]. HUVEC (3×10^4 cells/well) were incubated with PTX, PGA, E-[c(RGDfK)$_2$] and c(RADfK), combinations thereof, and with PGA-PTX-E-[c(RGDfK)$_2$] and PGA-PTX-c(RADfK) conjugates in EGM-2 medium. Following 8 h incubation, the wells were imaged and analyzed using NIH imageJ software.

In vivo tumor targeting evaluation

BALB/c female mice were inoculated to the mammary fat pad with 1×10^6 4T1 cells. Mice bearing 1 cm^3 tumors were treated i.v. with PGA-Cy5.5, PGA-c(RADfK)-Cy5.5 and PGA-E-[c(RGDfK)$_2$]-Cy5.5 at 50 μM RGD-equivalent concentration (n=3 mice/group).

CRI Maestro™ non-invasive intravital fluorescence imaging system was used to follow tumor accumulation. Mice were anesthetized using ketamine (100 mg/kg) and xylazine (12 mg/kg), treated with a depilatory cream (Veet®) and placed inside the imaging system at

different times (0, 1, 3, 7 and 22 h after treatment). Multispectral image-cubes were acquired through 590–750 nm spectral range in 10 nm steps using excitation (605 nm) and emission (635 nm) filter set. Mice auto fluorescence and undesired background signals were eliminated by spectral analysis and the Maestro™ linear unmixing algorithm.

Evaluation of antitumor activity and toxicity of the conjugates

BALB/c female mice were inoculated to the mammary fat pad with 1×10^6 4T1 cells. Mice bearing ~18 mm^3 tumors were treated i.v. with PTX, PGA, PTX vehicle (Ethanol:CremophorEL:Saline 1:1:8), PGA-PTX-c(RADfK) and PGA-PTX-E-[c(RGDfK)$_2$] conjugates at 15 mg/kg PTX-equivalent dose, every day (q.d.) for 5 days. Tumor progression was monitored by caliper measurement (width^2 × length × 0.52). Body weight and tumor size were monitored q.o.d. (n=5 mice/group).

Statistical methods

Data were expressed as mean ±SD for *in vitro* assays or ±SEM for *in vivo*. Statistical significance was determined using an unpaired *t*-test. All statistical tests were two-sided.

RESULTS

1. Physico-chemical characterization of the conjugates

1.1 Molecular weight, drug loading and polydispersity—The general two step synthesis of a PGA-PTX-E-[c(RGDfK)$_2$] is depicted in Figure 1A. The ester linker is hydrolytically labile. A series of PGA-based conjugates with general chemical structure (Figure 1A,C) has been synthesized and fully characterized. Average molecular weight (Mw) and polydispersity (Mw/Mn) were determined by size exclusion chromatography (SEC) as 17700 Da (Mw/Mn=1.3) for PGA, 48600 Da (Mw/Mn=1.3) for PGA-PTX-E-[c(RGDfK)$_2$] conjugate and 35700 Da (Mw/Mn=1.3) for PGA-E-[c(RGDfK)$_2$] conjugate.

Drug loading was determined by amino acid analysis, UV-Vis and HPLC (Figure 1E). PTX loading was determined in the range of 6.7 – 8.5 mol% and peptide loading from 4.8 to 5.6 mol% with a free drug content always less than 1.2 wt% of the total drug.

1.2 Hydrodynamic diameter of the conjugates—We characterized the hydrodynamic diameter and size distribution of our polydispersed population of peptide-bearing-PGA-PTX conjugates. Similar hydrodynamic diameter was demonstrated for PGA-PTX-E-[c(RGDfK)$_2$] conjugate (~7.7 nm), PGA-PTX-c(RADfK) control conjugate (~7.1 nm) and PGA-PTX control conjugate (~6.8 nm) (Figure 1B,D). All conjugates' sizes tone with those required for preferred tumor accumulation by the EPR effect.

2. Stability of the conjugates in plasma in the presence or absence of cathepsin B

Drug release profile and polymer degradation kinetics upon incubation with acetate buffer and cathepsin B were evaluated. Preliminary release studies of PTX from the conjugates exhibited time-dependent release kinetics (Figure 2A). Analysis of conjugates' stability in plasma (data not shown) revealed non-significant PTX release. In all cases, the main metabolite released from the polymer was PTX, as determined by LC/MS experiments using a MALDI-TOF as the MS detector.

3. Evaluation of toxicity of PGA-PTX-E-[c(RGDfK)$_2$] conjugate

Having shown that PTX is not released from the conjugate in plasma, we wanted to assess the biocompatibility of the conjugate in an RBC hemolysis assay [19]. The results clearly show that at concentrations up to 1 mg/mL, our polymers were not hemolytic *ex vivo* (Figure

2B) and therefore adequate for i.v. administration. In addition, the results show that usage of Cremophor EL, essential for free (insoluble) PTX administration, causes low hemolytic effect, emphasizing the advantages for PGA-conjugation of PTX that solubilizes it and allows its administration in saline.

4. Evaluation of OG-labeled-E-[c(RGDfK)$_2$] conjugate binding to $\alpha_v\beta_3$-expressing HUVEC

To evaluate the interaction between E-[c(RGDfK)$_2$] and $\alpha_v\beta_3$-expressing cells, we determined the expression levels of $\alpha_v\beta_3$ integrin on the cells using FACS. We confirmed that $\alpha_v\beta_3$ integrin is highly expressed on proliferating HUVEC cells (Figure 3A).

Using the Amnis ImageStream 100, we traced the interaction between E-[c(RGDfK)$_2$] and $\alpha_v\beta_3$ integrin by comparing fluorescence of the PGA-E-[c(RGDfK)$_2$]-OG and PGA-c(RADfK)-OG-labeled conjugates. Following incubation of 15 min, the ratio calculated for fluorescently-labeled PGA-E-[c(RGDfK)$_2$]-OG to PGA-c(RADfK)-OG-treated cells was 2.12 ± 0.28 (Figure 3B), indicating a faster cellular internalization via $\alpha_v\beta_3$ integrin.

5. Evaluation of the anti-angiogenic activity of PGA-PTX-E-[c(RGDfK)$_2$] conjugate

5.1 Evaluation of the effect of E-[c(RGDfK)$_2$]-bearing conjugates on HUVEC adhesion to fibrinogen—An endothelial cell adhesion assay was performed in order to evaluate the targeting specificity of E-[c(RGDfK)$_2$] conjugated with PTX and PGA by binding to $\alpha_v\beta_3$ integrin. As expected, free RGD–PM abrogated HUVEC adhesion at 50 μM by ~50%, while at the same concentration the free c(RADfK) peptide had no effect on the adhesion of the cells. PGA-PTX-E-[c(RGDfK)$_2$] conjugate (at 50 μM RGD-equivalent concentration) were able to inhibit HUVEC adhesion to fibrinogen by ~60% (Figure 3C). Free PTX, had a strong toxic effect on cells consequently the high concentration of the loaded PTX (~172.5 μM PTX), despite the very short exposure. PGA-PTX and PGA-PTX-c(RADfK) control conjugates (at PTX-equivalent concentration) had a minor inhibitory effect of ~10% and ~20% (respectively) on cell adhesion, indicating that conjugated PTX is not toxic to the cells as the free drug. Free PGA, had a negligible effect on endothelial cell adhesion.

5.2 Evaluation of the anti-proliferative effect of PGA-PTX-RGD-PM conjugate on HUVEC—HUVEC viability was evaluated following 72 h treatment with the different conjugates. Treatment with free PTX, had an IC_{50} value of 2.2 nM. Expectedly, as PTX-equivalent concentrations were used, PGA-PTX, PGA-PTX-c(RADfK) and PGA-PTX-E-[c(RGDfK)$_2$] conjugates had a similar IC_{50} value, of ~0.1 nM for the control conjugates and ~2.2 nM for the latter (Figure 3D). The combined free drugs (PTX and E-[c(RGDfK)$_2$]) exhibited similar activity as the free PTX alone (data not shown).

5.3 Evaluation of the effect of PGA-PTX-E-[c(RGDfK)$_2$] conjugate on HUVEC migration towards VEGF and their ability to form capillary-like tubes—Having shown that our conjugate has anti-angiogenic potential by inhibiting the proliferation and adhesion of HUVEC, we wanted to establish its ability to inhibit two important steps in the angiogenic cascade: migration towards VEGF and capillary-like tube formation of endothelial cells. The latter aims to imitate the capability of endothelial cells to form vascular networks *in vivo*.

PGA-PTX-E-[c(RGDfK)$_2$] conjugate at PTX-equivalent concentrations of 100 nM, inhibited the migration of HUVEC towards VEGF by ~50%. PTX alone, PGA-PTX and PGA-PTX-c(RADfK) conjugates showed slightly lower inhibitory effect of ~35–40%. PGA served as control and had neglect effect of ~10% inhibition (Figure 3E).

PGA-PTX-E-[c(RGDfK)$_2$] conjugate, PGA-PTX-c(RADfK) conjugate, free PTX and PGA-PTX at PTX-equivalent, low anti-angiogenic concentrations of 10 nM inhibited the formation of tubular structures of HUVEC by ~20% (Figure 3F). PGA had no significant effect on the formation of a vascular network.

We conclude that the conjugation of E-[c(RGDfK)$_2$] to PGA-PTX maintains and even strengthens its anti-angiogenic potential.

6. PGA-PTX-E-[c(RGDfK)$_2$] conjugate: Anticancer properties

The conjugate's advantage over free PTX or its control conjugate bearing RAD- PM was evaluated by targeting $\alpha_v\beta_3$-expressing cancer cells and inhibiting their growth.

We first determined the expression levels of $\alpha_v\beta_3$ integrin on U87-MG cell line using FACS and found that $\alpha_v\beta_3$ integrin is highly expressed on these cells (Figure 4A).

6.1 Evaluation of the anti-proliferative effect of E-[c(RGDfK)$_2$]-bearing conjugate on $\alpha_v\beta_3$ integrin-expressing cancer cells—

Free PTX, PGA-PTX and PGA-PTX-c(RADfK) control conjugates at PTX-equivalent doses, had a low effect on $\alpha_v\beta_3$-expressing U87-MG cells, exhibiting an IC_{50} value of more than 10000 nM, higher than what was observed for the HUVEC. Moreover, PGA-PTX-E-[c(RGDfK)$_2$] exhibited a different IC_{50} value of ~4000 nM PTX-equivalent indicating improved effect on the cells (Figure 4B). The combined free drugs exhibited similar activity as the free PTX alone (data not shown).

6.2 Intracellular uptake of OG-labeled-RGD-PM conjugate—

U87-MG cells were incubated for 1 h with OG-labeled conjugates, fixed, permeabilized and stained with phalloidin (red) for actin filaments. Confocal microscopy analysis revealed that RGD-containing conjugate accumulates in the cytoplasm of the cells, as opposed to RAD-containing conjugate, which was not detected at these concentrations (Figure 4C).

In vivo evaluation of the targeting ability of RGD-bearing conjugates was also performed. Confocal microscopy analysis of mCherry–labeled-U87-MG tumors or FACS sorting of mCherry–labeled-MG-63 human osteosarcoma (see supplementry data) dissected from mice treated with PGA-E-[c(RGDfK)$_2$]-OG revealed accumulation of the conjugate at the tumor site, targeting $\alpha_v\beta_3$-expressing tumor and endothelial cells as opposed to the PGA-c(RADfK)-OG or PGA-OG conjugates (Figure 4D and figure S1) that could not be detected at these concentrations.

7. *In vivo* antitumor efficacy and toxicity evaluation of PGA-PTX-E-[c(RGDfK)$_2$] conjugate

In order to evaluate the conjugate's anti-angiogenic and antitumor efficacy *in vivo*, we inoculated orthotopically aggressive, fast-growing murine 4T1 breast cancer cells into the mammary fat pad of Balb/C mice [32]. 4T1 cells express low levels of $\alpha_v\beta_3$ integrin, as was determined by PCR. Normal expression level of the α_v subunit combined with low expression of the limiting β_3 subunit (Figure 5A) indicates that the cells express low levels of the integrin; hence the activity of the conjugate at the tumor site will be dominated by its anti-angiogenic activity on the proliferating endothelial cells expressing the target integrin.

A 72 h proliferation assay was performed in order to evaluate 4T1 cells sensitivity to PTX or PGA-PTX-E-[c(RGDfK)$_2$]. Surprisingly, the IC_{50} found for both free PTX and the PGA-PTX-E-[c(RGDfK)$_2$] conjugate was equal at ~45 nM, whereas the control PGA-PTX and PGA-PTX-c(RADfK) conjugates were less toxic to the cells with an IC_{50} of ~210 nM. The

combined free drugs exhibited similar activity as the free PTX alone (data not shown) and PGA had no effect on the cells (Figure 5B).

Preferable active targeting and accumulation of the PGA-PTX-E-[c(RGDfK)$_2$] conjugate at 4T1 tumor site was evaluated *in vivo* using the Maestro™ imaging system. 4T1-tumor-bearing mice were treated with PGA-E-[c(RGDfK)$_2$]-Cy5.5, PGA-c(RADfK)-Cy5.5 or PGA-Cy5.5 and the fluorescence was measured at different times (0, 1, 3, 7 and 22 h). For each mouse, the conjugate accumulation at the tumor site was calculated (Figure 5C). All conjugates were passively targeted to the tumor site by the EPR effect, yet the PGA-E-[c(RGDfK)$_2$] conjugate showed preferred time-dependent accumulation at the tumor site. Maximal accumulation of the conjugates was 7 h after treatment (Figure 5D) and 22 h after treatment all conjugates fluorescence was diminished, indicating clearance of the conjugates.

Tumor growth inhibition by PGA-PTX-E-[c(RGDfK)$_2$] conjugate was enhanced (T/C=0.59) compared with that seen for free PTX (T/C=0.82), PGA-PTX (T/C=0.84) or PGA-PTX-c(RADfK) control (T/C=0.86). Tumor progression was demonstrated with control groups treated with PGA or PTX-vehicle at PTX-equivalent dose (Figure 6A). Mice were treated with free PTX, PTX vehicle, PGA, the conjugates PGA-PTX, PGA-PTX-c(RADfK) or PGA-PTX-E-[c(RGDfK)$_2$] at concentrations of 15 mg/kg PTX q.d. Treatment was detained after 5 days due to high toxicity of free PTX, indicated by severe weight loss and demise of 3 mice, whereas conjugate-treated mice continued to gain weight normally (Figure 6B). Since PGA-PTX-E-[c(RGDfK)$_2$] exhibited superior safety over PTX and PGA-PTX, we conclude that a higher dose of our conjugate can be used in future *in vivo* experiments.

DISCUSSION

Two successful strategies in cancer therapy that are currently being evaluated in clinical trials consist of targeting $\alpha_v\beta_3$ integrin receptors and conjugating PTX to a polymer. However, the thought of combining these powerful approaches by developing an anti-$\alpha_v\beta_3$ and PTX bi-specific macromolecule targeting the tumor cells and their endothelial microenvironment had not been given previous consideration. The synergism found here, results in a therapy that constitutes a significant step within the field.

The potent $\alpha_v\beta_3/\alpha_v\beta_5$ inhibitor c(RGDf[NMe]V), known as Cilengitide, was the first to target the integrin, as an anti-angiogenic therapy [33, 34]. The clinical potential of Cilengitide (EMD121974) was recognized and presently, Cilengitide is tested in several clinical trials as monotherapy or in combination with conventional chemotherapy [35–37]. Despite the reported clinical advances of Cilengitide, it was recently reported in two distressing publications that RGD-mimetic agents, at well-defined experimental setting, may promote, rather than inhibit, angiogenesis [38].

Opaxio™, a PGA–PTX conjugate, is currently undergoing phase III clinical trials showing promising results [15–17] and it is expected to be the first polymer-drug conjugate to reach the market in the near future.

Here we described the design, synthesis and characterization of a biodegradable water-soluble PGA-PTX-E-[c(RGDfK)$_2$] conjugate that targets $\alpha_v\beta_3$ integrin-overexpressed at the tumor site. A library of PGA conjugates bearing PTX, E-[c(RGDfK)$_2$] and their combinations was synthesized to contain PTX and peptides up to a 8.6 and 5.6 mol % loading, respectively. The hydrophilicity of the PGA and the hydrophobicity of the PTX favor the formation of compact unimolecular micelles as shown by DLS. The size of the

micelles (~ 10 nm diameter) suggests the formation of unimolecular micelles, where the PTX hydrophobic nature leads the compaction of the conjugate.

Effective biological activity of polymer-drug conjugates relies on (i) the stability in blood circulation and (ii) the lysosomal enzyme cleavage to release the active drug inside the target cells following cellular uptake. The PGA conjugates were stable in plasma, but were degraded in the presence of lysosomal cathepsin B, releasing the drug in a time-dependent manner.

Comparing the anti-angiogenic activity of the conjugates on HUVEC, overexpressing $\alpha_v\beta_3$ integrin and interacting with E-[c(RGDfK)$_2$], by both adhesion and proliferation assays supported the published advantage for the bis-cyclic RGD-bearing conjugates, demonstrating greater adhesion to fibrinogen properties [31, 39]. E-[c(RGDfK)$_2$] was previously used either as direct inhibitor or as targeting moiety [31, 39–41] and in this study we further demonstrate that the conjugation of E-[c(RGDfK)$_2$] with PGA-PTX does not abrogate its inhibitory ability on adhesion of endothelial cells to fibrinogen.

In addition, the anti-angiogenic effect of PGA-PTX-E-[c(RGDfK)$_2$] on HUVEC was demonstrated by tube-formation and migration assays. The conjugate exhibited anti-angiogenic effect, yet less effective than free PTX. The logical explanation lies with the amount of free drug available to the cells *in vitro*. PTX release from the conjugate, hence, its effect, depends on the kinetics of an enzymatic reaction; therefore, the concentration of free drug available to the cells is lower for the conjugated PTX at any given time. However, it is clear that PTX is efficiently released from the conjugate and shows a significant inhibitory effect.

No significant difference between PGA-PTX-E-[c(RGDfK)$_2$] and the PTX-conjugated controls was observed in the proliferation, migration and capillary-like tube formation assays, because RGD-targeting has no advantage *in vitro*.

Notably, we showed that E-[c(RGDfK)$_2$] functions as a targeting moiety both *ex vivo* and *in vivo*. Following intravenous injection, the conjugate travels in the vessels and passively extravasates at the tumor site because of the EPR effect, but it also actively binds to receptor overexpressing cells.

The anticancer activity of our conjugate was demonstrated, proving our hypothesis that it will have an advantage on $\alpha_v\beta_3$ integrin-overxpressing cancers. We demonstrate that U87-MG cells overexpress $\alpha_v\beta_3$ integrin and adhere to our E-[c(RGDfK)$_2$]-bearing conjugate. Consequently, the conjugate inhibits their proliferation more effectively than free PTX.

Both the conjugation of PTX with PGA carrier and the addition of a targeting moiety were designed to alter and improve PTX efficacy and minimize its side effects. Another aspect that can be challenged by this conjugation is overcoming PTX-acquired resistance. PTX is an effective therapy for breast cancer; however, sensitivity to PTX varies among patients. PTX-resistance is suspected to be related to the up-regulation of $\alpha_v\beta_3$ and its signaling pathway [42], hence, targeting the drug to the cells via this receptor, holds a promise to manipulate the efflux pumps' related resistance. Moreover, anti-angiogenic therapy had been suggested as an alternative to overcome drug resistant.

As a first step we tested whether the inhibitory effect of our PGA-PTX-E-[c(RGDfK)$_2$] conjugate on the proliferation of 4T1 murine breast cancer cells differs from free PTX or PGA-PTX. Although 4T1 do not express high levels of the $\alpha_v\beta_3$ integrin, PGA-PTX-E-[c(RGDfK)$_2$] had an inhibitory effect on these cells as did free PTX. By using fluorescent tagging of the conjugates, we were able to show selective accumulation of the RGD-bearing

conjugate in the 4T1 tumor site, indicating an advantage for the actively targeted conjugate over the control conjugates, directed by the EPR effect alone. Moreover, the accrual of PGA-PTX-E-[c(RGDfK)$_2$] in a non-expressing $\alpha_v\beta_3$ integrin tissue imply that the conjugate was directed to the proliferating endothelial cells in the growing tumor, and that the effect seen for the conjugate, in that case, is mostly anti-angiogenic. Our preliminary *in vivo* study, treating highly aggressive 4T1 tumors for a short period of 5 days with PTX was able to show improved antitumor effect for the conjugate versus free PTX or PGA-PTX, together with lower toxic side effects. These preliminary results pave the way for future studies using escalating doses of the conjugate and determining its maximum tolerated dose (MTD). We are currently investigating the mechanism of overcoming PTX resistance; however, this ongoing work lies outside of the scope of this article.

By showing the advantages of our multivalent polymeric conjugate which alters the pharmacokinetics of the free drug, we hope to warrant it as a novel targeted, anti-angiogenic and anticancer therapy.

Conclusions

The targeted polymer-based PTX delivery conjugate, PGA-PTX-E-[c(RGDfK)$_2$], significantly augments the antitumor activity of both the free drug and the conjugated PGA-PTX. Inclusion of an active targeting moiety to integrin expressing-cells, leads to a selective anti-angiogenic mechanism of action and an alternative manipulation to overcome acquired multi-drug resistance.

Supplementary Material

Refer to Web version on PubMed Central for supplementary material.

Acknowledgments

This research was supported by THE ISRAEL SCIENCE FOUNDATION (Grant No. 1300/06), by the Israel Cancer Association, by the Recanati Foundation (RSF) and by the United States-Israel Binational Science Foundation (Grant No. 2007347, RSF and RL). We thank the Spanish Ministry of Science and Education (MICINN, CTQ 2007-060601), Generalitat Valenciana (ACOMP/2009/086), European Commission FP7-Health program (proposal n° 241919, LIVIMODE) and Centro de Investigación Príncipe Felipe for their financial support. MJV is a Ramón y Cajal researcher. This research was supported in part by NIH grant R01 CA118975 (RL). We would also like to thank Markel Technologies, David Golan and Ariel Roytman for their kind assistance using the ImageStream Multispectral Imaging flow Cytometer.

References

1. Folkman, J. History of angiogenesis. In: Figg, W.; Folkman, J., editors. Angiogenesis: an integrative approach from science to medicine. Heidelberg, Germany: Springer-Verlag; 2008. p. 1-14.
2. Folkman J. Angiogenesis: an organizing principle for drug discovery? Nat Rev Drug Discov. 2007; 6(4):273–86. [PubMed: 17396134]
3. Alavi, SA.; Cheresh, DA. Integrins in angiogenesis. In: Figg, W.; Folkman, J., editors. Angiogenesis: an integrative approach from science to medicine. Heidelberg, Germany: Springer-Verlag; 2008. p. 63-73.
4. Cox D, Aoki T, Seki J, Motoyama Y, Yoshida K. The pharmacology of the integrins. Med Res Rev. 1994; 14(2):195–228. [PubMed: 8189836]
5. Avraamides CJ, Garmy-Susini B, Varner JA. Integrins in angiogenesis and lymphangiogenesis. Nat Rev Cancer. 2008; 8(8):604–17. [PubMed: 18497750]
6. Stromblad S, Cheresh DA. Integrins, angiogenesis and vascular cell survival. Chem Biol. 1996; 3(11):881–5. [PubMed: 8939711]

7. Bazzoni G, Dejana E, Lampugnani MG. Endothelial adhesion molecules in the development of the vascular tree: the garden of forking paths. Curr Opin Cell Biol. 1999; 11(5):573–81. [PubMed: 10508655]
8. Lohof E, Planker E, Mang C, Burkhart F, Dechantsreiter MA, Haubner R, et al. Carbohydrate derivatives for use in drug design:cyclic alpha(v)-selective RGD peptides. Angew Chem Int Ed Engl. 2000; 39(15):2761–4. [PubMed: 10934419]
9. Monferran S, Skuli N, Delmas C, Favre G, Bonnet J, Cohen-Jonathan-Moyal E, et al. Alphavbeta3 and alphavbeta5 integrins control glioma cell response to ionising radiation through ILK and RhoB. Int J Cancer. 2008; 123(2):357–64. [PubMed: 18464290]
10. Felding-Habermann B, Mueller BM, Romerdahl CA, Cheresh DA. Involvement of integrin alpha V gene expression in human melanoma tumorigenicity. J Clin Invest. 1992; 89(6):2018–22. [PubMed: 1376331]
11. Wang J, Lou P, Lesniewski R, Henkin J. Paclitaxel at ultra low concentrations inhibits angiogenesis without affecting cellular microtubule assembly. Anticancer Drugs. 2003; 14(1):13–9. [PubMed: 12544254]
12. Miele E, Spinelli GP, Miele E, Tomao F, Tomao S. Albumin-bound formulation of paclitaxel (Abraxane ABI-007) in the treatment of breast cancer. Int J Nanomedicine. 2009; 4:99–105. [PubMed: 19516888]
13. Gradishar WJ. Albumin-bound paclitaxel: a next-generation taxane. Expert Opin Pharmacother. 2006; 7(8):1041–53. [PubMed: 16722814]
14. Miller K, Erez R, Segal E, Shabat D, Satchi-Fainaro R. Targeting bone metastases with a bispecific anticancer and antiangiogenic polymer-alendronate-taxane conjugate. Angew Chem Int Ed Engl. 2009; 48(16):2949–54. [PubMed: 19294707]
15. Langer CJ, O'Byrne KJ, Socinski MA, Mikhailov SM, Lesniewski-Kmak K, Smakal M, et al. Phase III trial comparing paclitaxel poliglumex (CT-2103, PPX) in combination with carboplatin versus standard paclitaxel and carboplatin in the treatment of PS 2 patients with chemotherapy-naive advanced non-small cell lung cancer. J Thorac Oncol. 2008; 3(6):623–30. [PubMed: 18520802]
16. Paz-Ares L, Ross H, O'Brien M, Riviere A, Gatzemeier U, Von Pawel J, et al. Phase III trial comparing paclitaxel poliglumex vs docetaxel in the second-line treatment of non-small-cell lung cancer. Br J Cancer. 2008; 98(10):1608–13. [PubMed: 18475293]
17. O'Brien ME, Socinski MA, Popovich AY, Bondarenko IN, Tomova A, Bilynsky BT, et al. Randomized phase III trial comparing single-agent paclitaxel poliglumex (CT-2103, PPX) with single-agent gemcitabine or vinorelbine for the treatment of PS 2 patients with chemotherapy-naive advanced non-small cell lung cancer. J Thorac Oncol. 2008; 3(7):728–34. [PubMed: 18594318]
18. Buescher JM, Margaritis A. Microbial biosynthesis of polyglutamic acid biopolymer and applications in the biopharmaceutical, biomedical and food industries. Crit Rev Biotechnol. 2007; 27(1):1–19. [PubMed: 17364686]
19. Duncan R, Ferruti P, Sgouras D, Tuboku-Metzger A, Ranucci E, Bignotti F. A polymer-Triton X-100 conjugate capable of PH-dependent red blood cell lysis: a model system illustrating the possibility of drug delivery within acidic intracellular compartments. J Drug Target. 1994; 2(4): 341–7. [PubMed: 7858959]
20. Vicent MJ, Perez-Paya E. Poly-L-glutamic acid (PGA) aided inhibitors of apoptotic protease activating factor 1 (Apaf-1): an antiapoptotic polymeric nanomedicine. J Med Chem. 2006; 49(13):3763–5. [PubMed: 16789732]
21. Strojnik T, Zajc I, Bervar A, Zidanik B, Golouh R, Kos J, et al. Cathepsin B and its inhibitor stefin A in brain tumors. Pflugers Arch. 2000; 439(3 Suppl):R122–3. [PubMed: 10653164]
22. Strojnik T, Kos J, Zidanik B, Golouh R, Lah T. Cathepsin B immunohistochemical staining in tumor and endothelial cells is a new prognostic factor for survival in patients with brain tumors. Clin Cancer Res. 1999; 5(3):559–67. [PubMed: 10100707]
23. Decock J, Obermajer N, Vozelj S, Hendrickx W, Paridaens R, Kos J. Cathepsin B, cathepsin H, cathepsin X and cystatin C in sera of patients with early-stage and inflammatory breast cancer. Int J Biol Markers. 2008; 23(3):161–8. [PubMed: 18949742]

24. Foekens JA, Kos J, Peters HA, Krasovec M, Look MP, Cimerman N, et al. Prognostic significance of cathepsins B and L in primary human breast cancer. J Clin Oncol. 1998; 16(3):1013–21. [PubMed: 9508185]
25. Haag R, Kratz F. Polymer therapeutics: concepts and applications. Angew Chem Int Ed Engl. 2006; 45(8):1198–215. [PubMed: 16444775]
26. Satchi-Fainaro R, Puder M, Davies JW, Tran HT, Sampson DA, Greene AK, et al. Targeting angiogenesis with a conjugate of HPMA copolymer and TNP-470. Nat Med. 2004; 10(3):255–61. [PubMed: 14981512]
27. Satchi-Fainaro R, Mamluk R, Wang L, Short SM, Nagy JA, Feng D, et al. Inhibition of vessel permeability by TNP-470 and its polymer conjugate, caplostatin. Cancer Cell. 2005; 7(3):251–61. [PubMed: 15766663]
28. Segal E, Pan H, Ofek P, Udagawa T, Kopeckova P, Kopecek J, et al. Targeting angiogenesis-dependent calcified neoplasms using combined polymer therapeutics. PLoS One. 2009; 4(4):e5233. [PubMed: 19381291]
29. Curtin SA, Deming TJ. Initiators for end-group functionalized polypeptides via tandem addition reactions. J Am Chem Soc. 1999; 121(32):7427–8.
30. Polyak D, Ryppa C, Eldar-Boock A, Ofek P, Many A, Licha K, et al. Development of PEGylated doxorubicin-E-[c(RGDfK)$_2$] conjugate for integrin-targeted cancer therapy. Polym Adv Technol. 2011; 22:103–13.
31. Ryppa C, Mann-Steinberg H, Biniossek ML, Satchi-Fainaro R, Kratz F. In vitro and in vivo evaluation of a paclitaxel conjugate with the divalent peptide E-[c(RGDfK)2] that targets integrin alpha v beta 3. Int J Pharm. 2009; 368(1–2):89–97. [PubMed: 18992308]
32. Liu Z, Chen K, Davis C, Sherlock S, Cao Q, Chen X, et al. Drug delivery with carbon nanotubes for in vivo cancer treatment. Cancer Res. 2008; 68(16):6652–60. [PubMed: 18701489]
33. Dechantsreiter MA, Planker E, Matha B, Lohof E, Holzemann G, Jonczyk A, et al. N-Methylated cyclic RGD peptides as highly active and selective alpha(V)beta(3) integrin antagonists. J Med Chem. 1999; 42(16):3033–40. [PubMed: 10447947]
34. Aumailley M, Gurrath M, Muller G, Calvete J, Timpl R, Kessler H. Arg-Gly-Asp constrained within cyclic pentapeptides. Strong and selective inhibitors of cell adhesion to vitronectin and laminin fragment P1. FEBS Lett. 1991; 291(1):50–4. [PubMed: 1718779]
35. NIH. http://clinicaltrials.gov/search/intervention=Cilengitide. Available from: http://clinicaltrials.gov/search/intervention=Cilengitide
36. Paolillo M, Russo MA, Serra M, Colombo L, Schinelli S. Small molecule integrin antagonists in cancer therapy. Mini Rev Med Chem. 2009; 9(12):1439–46. [PubMed: 19929817]
37. Desgrosellier JS, Cheresh DA. Integrins in cancer: biological implications and therapeutic opportunities. Nat Rev Cancer. 2010; 10(1):9–22. [PubMed: 20029421]
38. Reynolds AR, Hart IR, Watson AR, Welti JC, Silva RG, Robinson SD, et al. Stimulation of tumor growth and angiogenesis by low concentrations of RGD-mimetic integrin inhibitors. Nat Med. 2009; 15(4):392–400. [PubMed: 19305413]
39. Mitra A, Mulholland J, Nan A, McNeill E, Ghandehari H, Line BR. Targeting tumor angiogenic vasculature using polymer-RGD conjugates. J Control Release. 2005; 102(1):191–201. [PubMed: 15653145]
40. Park K, Kim YS, Lee GY, Park RW, Kim IS, Kim SY, et al. Tumor endothelial cell targeted cyclic RGD-modified heparin derivative: inhibition of angiogenesis and tumor growth. Pharm Res. 2008; 25(12):2786–98. [PubMed: 18581207]
41. Ryppa C, Mann-Steinberg H, Fichtner I, Weber H, Satchi-Fainaro R, Biniossek ML, et al. In vitro and in vivo evaluation of doxorubicin conjugates with the divalent peptide E-[c(RGDfK)2] that targets integrin alphavbeta3. Bioconjug Chem. 2008
42. Vellon L, Menendez JA, Liu H, Lupu R. Up-regulation of alphavbeta3 integrin expression is a novel molecular response to chemotherapy-induced cell damage in a heregulin-dependent manner. Differentiation. 2007; 75(9):819–30. [PubMed: 17999741]

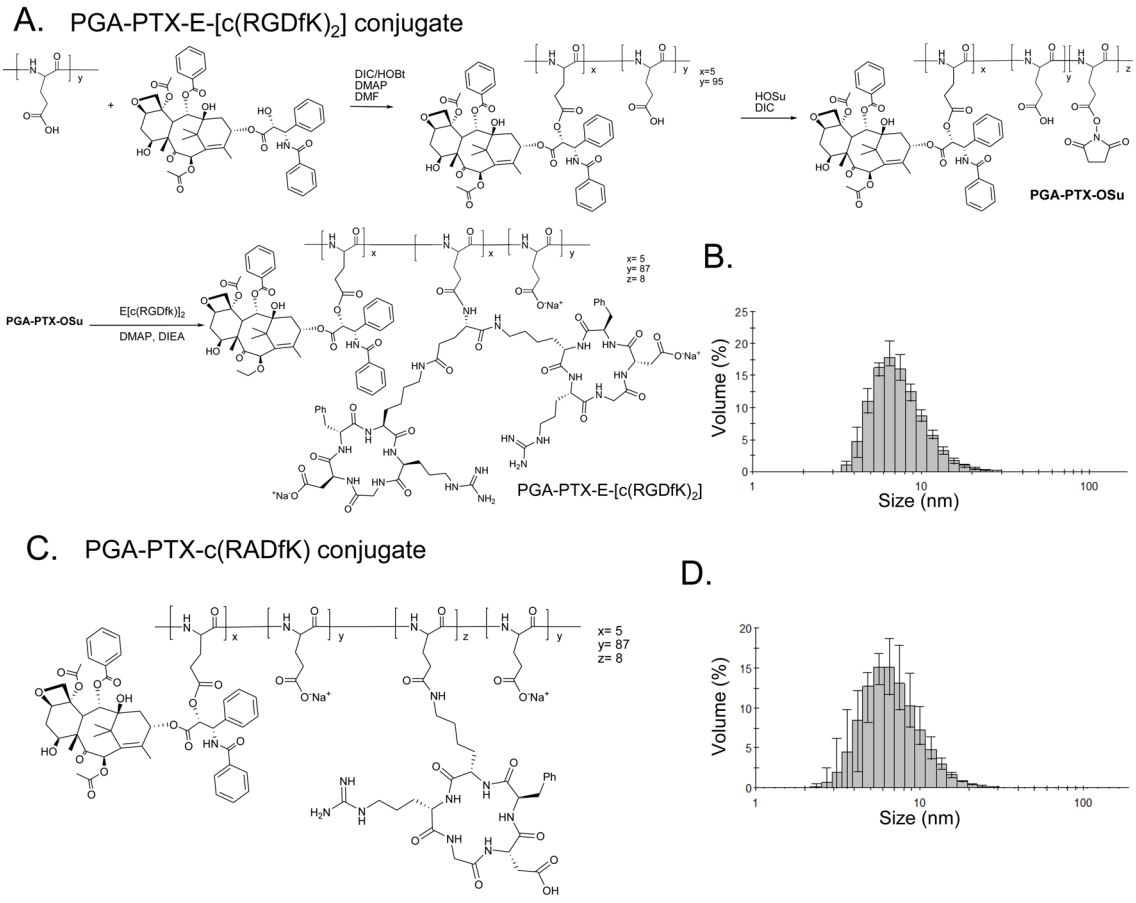

E.

Conjugate	Total PTX loading (mol%) [a]	Total peptide loading (mol %) [b]	Free drug content (wt % of total drug)[c] PTX	Peptide	Hydrodynamic diameter (nm)
PGA-PTX	6.7 ± 0.3	NA	1.2 ± 0.4	NA	6.8 ± 0.5
PGA-PTX-c(RADfK)	8.5 ± 0.3	4.8 ± 0.4	1.1 ± 0.3	0.7 ± 0.1	7.7 ± 0.1
PGA-PTX-E-[c(RGDfK)$_2$]	8.6 ± 0.3	4.9 ±0.2	1.1 ± 0.3	0.8 ± 0.2	7.1 ± 0.6

a. Determined by UV and HPLC; b. Determined by UV, HPLC and aminoacid analysis; c. Determined by HPLC. NA: not-appropriate

Figure 1.

(**A,B**) Chemical structures and Hydrodynamic diameters of PGA-PTX-E-[c(RGDfK)$_2$] (**C,D**) Chemical structures and Hydrodynamic diameters of PGA-PTX-c(RADfK). (**E**) Characterization of the synthesized conjugates.

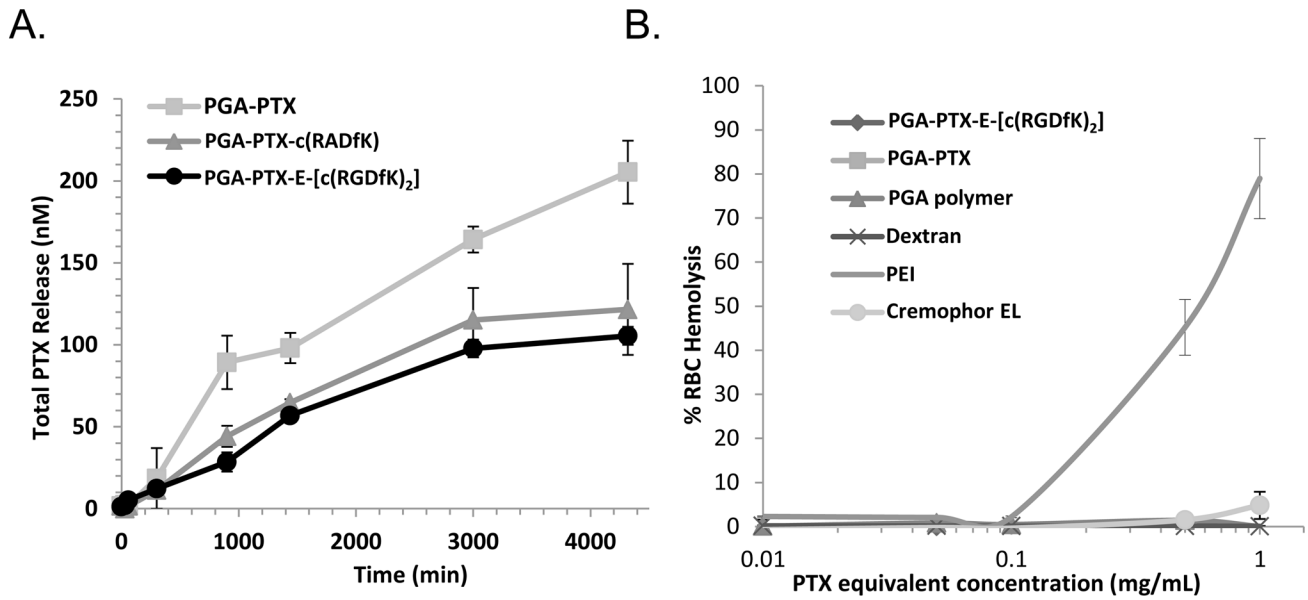

Figure 2. Characterization of PGA-PTX-E-[c(RGDfK)$_2$] conjugate

(**A**) PTX is released from the conjugates at distinct kinetics in the presence of cathepsin B at pH 6, at 37°C. **(B)** PGA-PTX-E-[c(RGDfK)$_2$] is non-toxic at the concentrations required for effective targeting *in vivo*. Red blood cell lysis assay of conjugate and controls. Data represents mean ± SD. Due to similar low values, some symbols overlap.

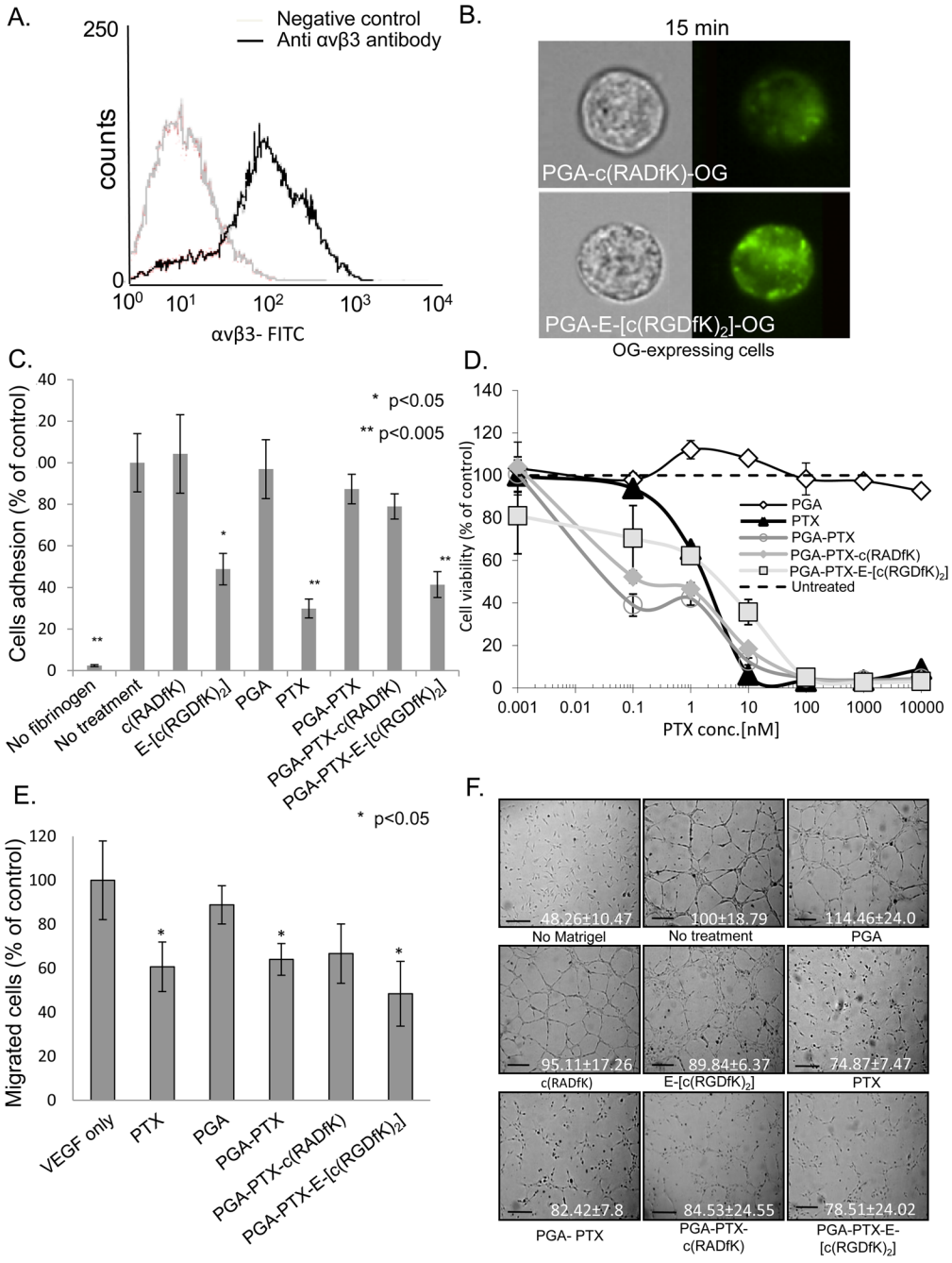

Figure 3. PGA-PTX-E-[c(RGDfK)$_2$] conjugate is anti-angiogenic

(A) HUVEC express $\alpha_v\beta_3$ integrin **(B)** PGA-E-[c(RGDfK)$_2$]-OG demonstrates preferred binding to $\alpha_v\beta_3$-expressing-HUVEC compared with control. **(C)** RGD-bearing conjugate inhibit the adhesion of HUVEC to fibrinogen. **(D)** PTX (IC_{50} 1.9 nM) and PGA-PTX-E-[c(RGDfK)$_2$] conjugate (~2.2 nM) inhibit HUVEC proliferation following 72 h incubation. **(E)** PGA-PTX-E-[c(RGDfK)$_2$] inhibited the migration of HUVEC towards the chemoattractant VEGF. **(F)** PGA-PTX-E-[c(RGDfK)$_2$] inhibited the formation of tubular structures of HUVEC. Representative images (bar=100 μm), quantitative analysis of the mean length of tubes is indicated.Data represents mean ± SD.

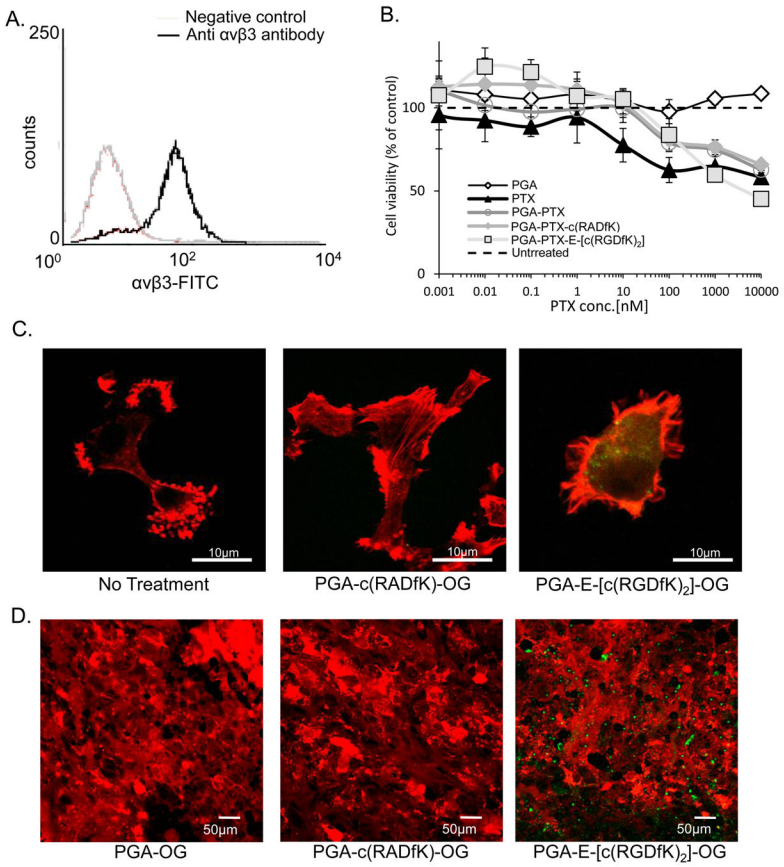

Figure 4. PGA-PTX-E-[c(RGDfK)$_2$] conjugate targets and inhibits the growth of $\alpha_v\beta_3$ integrin-expressing-cancer cells

(A) U87-MG express $\alpha_v\beta_3$ integrin. **(B)** PGA-PTX-E-[c(RGDfK)$_2$] inhibits the proliferation of U87-MG. Data represents mean ± SD. **(C)** PGA-E-[c(RGDfK)$_2$]-OG (green) binds preferably to U87-MG cells. Actin filaments were stained with phalloidin (red). **(D)** PGA-E-[c(RGDfK)$_2$]-OG conjugate selectively accumulate in U87-MG tumors *in vivo*.

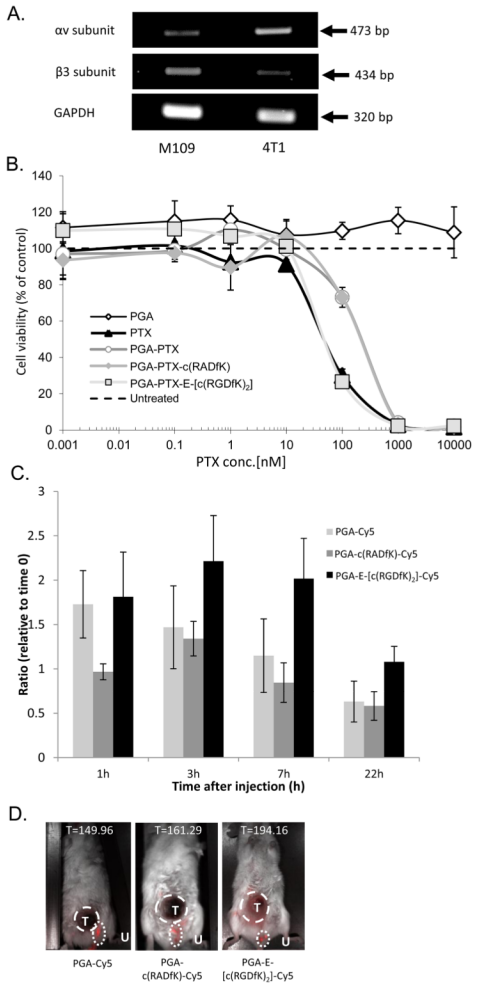

Figure 5.

(A) 4T1 cells express α_v integrin-subunit, but low β_3 integrin subunit, hence, very low expression of the $\alpha_v\beta_3$ integrin is expected. M109 murine cells were used as control. **(B)** PGA-PTX-E-[c(RGDfK)$_2$] inhibits the proliferation of 4T1 cells as free PTX. Data represents mean ± SD. **(C,D) PGA-PTX-E-[c(RGDfK)$_2$] conjugate accumulates in tumors.** 4T1 tumor-bearing mice were treated with Cy5.5-marked conjugates. PGA-E-[c(RGDfK)$_2$]-Cy5.5 conjugate selectively accumulate in 4T1 tumors *in vivo.* Data represents mean ± SEM. C- Conjugates' accumulation in tumors over time. D- Maximal accumulation was 7 h after treatment. Tumor area indicated by T, Urine remnant on the mouse fur represented by U and was not calculated. T= counts/sec/tumor area.

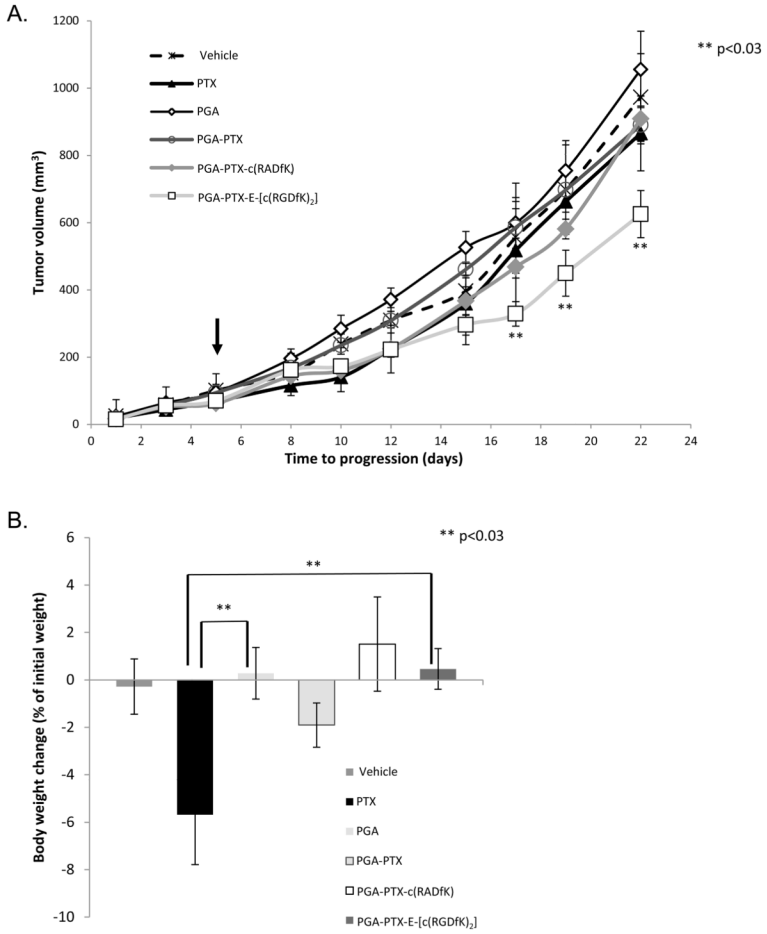

Figure 6. (A) PGA-PTX-E-[c(RGDfK)$_2$] conjugate inhibits tumor growth

PGA-PTX-E-[c(RGDfK)$_2$] conjugate inhibited tumor growth (arrow indicates end of treatment, n=5 mice/group). **(B)** PTX-treated mice showed signs of toxicity after 5 days of treatment, indicated by death of 2 mice and decrease in body weight. Data represents mean ± SEM.